Effects of hindlimb unloading and subsequent reloading on the structure and mechanical properties of Achilles tendon-to-bone attachment

Claire Camy, Thomas Brioche, Karim Senni, Alexandrine Bertaud, Cécile Genovesio, Edouard Lamy, Théo Fovet, Angèle Chopard, Martine Pithioux, Sandrine Roffino

Effects of hindlimb unloading and subsequent reloading on the structure and mechanical properties of Achilles tendon-to-bone attachment

Claire Camy[1] | Thomas Brioche[2] | Karim Senni[3] | Alexandrine Bertaud[4,5] | Cécile Genovesio[5] | Edouard Lamy[1,5] | Théo Fovet[2] | Angèle Chopard[2] | Martine Pithioux[1,6,7] | Sandrine Roffino[1,7]

[1]Aix Marseille University, CNRS, ISM, Institute of Movement Sciences, Marseille, France

[2]DMEM, Montpellier University, INRAE, UMR 866, Montpellier, France

[3]CNRS UMR 7244 CSPBAT Ingénierie Tissulaire et Protéomique, Bobigny, France

[4]Aix Marseille University, INSERM 1263, INRA 1260, C2VN, Marseille, France

[5]Laboratoire de Biochimie, Faculté de Pharmacie, Marseille, France

[6]APHM, Hôpital Sainte Marguerite, IML, Marseille, France

[7]Aix Marseille University, CNRS, ISM, Centrale Marseille, Mecabio Platform, Anatomic Laboratory, Timone, Marseille, France

Correspondence
Sandrine Roffino, Institut des Sciences du Mouvement UMR 7287, Parc Scientifique et Technologique de Luminy, 163, avenue de Luminy, Case Postale 91, 13288 Marseille Cedex 09, France.
Email: sandrine.roffino@univ-amu.fr

Funding information
Centre National d'Etudes Spatiales (CNES), Grant/Award Number: 4800000797

Abstract

While muscle and bone adaptations to deconditioning have been widely described, few studies have focused on the tendon enthesis. Our study examined the effects of mechanical loading on the structure and mechanical properties of the Achilles tendon enthesis. We assessed the fibrocartilage surface area, the organization of collagen, the expression of collagen II, the presence of osteoclasts, and the tensile properties of the mouse enthesis both after 14 days of hindlimb suspension (HU) and after a subsequent 6 days of reloading. Although soleus atrophy was severe after HU, calcified fibrocartilage (CFc) was a little affected. In contrast, we observed a decrease in non-calcified fibrocartilage (UFc) surface area, collagen fiber disorganization, modification of morphological characteristics of the fibrocartilage cells, and altered collagen II distribution. Compared to the control group, restoring normal loads increased both UFc surface area and expression of collagen II, and led to a crimp pattern in collagen. Reloading induced an increase in CFc surface area, probably due to the mineralization front advancing toward the tendon. Functionally, unloading resulted in decreased enthesis stiffness and a shift in site of failure from the osteochondral interface to the bone, whereas 6 days of reloading restored the original elastic properties and site of failure. In the context of spaceflight, our results suggest that care must be taken when performing countermeasure exercises both during missions and during the return to Earth.

KEYWORDS

Achilles tendon enthesis, collagen II, fibrocartilage, hindlimb suspension, mechanical properties, reloading

1 | INTRODUCTION

Maintaining the characteristics of the musculoskeletal system requires mechanical loading. Spaceflights place astronauts in a microgravity environment that affects their musculoskeletal system. The decreased loading induced by a real or simulated space environment has been shown to result in structural and functional alterations to muscles and bones, principally muscular atrophy, reduced muscle strength, and bone loss.[1–4] While significant effects on the structure, composition, and mechanical properties of tendons have been reported,[5–10] little is known about how microgravity affects tendon-to-bone attachment, also called enthesis. Yet understanding the responses of the structures involved in the production of force, as well as those that transmit it to the bone, is crucial both to prevent astronauts from suffering adverse effects during spaceflight and to optimize rehabilitation strategies when they return to the ground.

The enthesis is the specialized region where a tendon attaches to bone and as such plays an essential role in the transmission of force from tendon to bone.[11,12] The Achilles tendon enthesis, which transmits the force from the soleus and gastrocnemius muscles to the calcaneus, is a fibrocartilaginous enthesis.[13] The molecules that compose the enthesis and their organization allow stress to be dissipated and protect the structure from the risk of failure during the transmission of forces.[11,14] As collagens and minerals mainly determine the tensile properties of the interface,[12,15–16] proteoglycans (PG) reflect the compressive forces to which the enthesis is subjected and are thought to protect the enthesis against shear, wear, and tear.[12,17]

To date, Deymier et al. (2020)[6] is the only study to have investigated the effects of spaceflight on entheses. Whereas studies have demonstrated that entheses are sensitive to chronic variations in mechanical load,[18–23] Deymier et al. (2020)[6] reported that spaceflight did not mechanically weaken the supraspinatus tendon enthesis. However, the supraspinatus, a shoulder muscle, is documented as suffering little impact from microgravity.[24] Conversely, real and simulated microgravity is reported to lead to significant atrophy of the soleus and gastrocnemius muscles, decreasing the muscle force generated,[3] which reduces mechanical stress on the Achilles tendon enthesis. This unloading of the Achilles enthesis may induce a structural remodeling of this interface that could alter its mechanical properties and weaken it.

The goal of our study was to determine the effects of simulated microgravity on Achilles tendon enthesis structure, as well as its impact on tensile strength. We used the hindlimb unloading rodent model, commonly used to simulate weightlessness.[25] Mice were hindlimb-suspended for 2 weeks. The study investigated the calcified and uncalcified fibrocartilage surface areas, the organization of collagen fibers, the expression of collagen II, and the plasticity of the interfaces (mineralization front and osteochondral junction). Hypothesizing that unloading would involve structural remodeling with functional consequences, we assessed the elastic properties of unloaded entheses as well as their tensile strength. Moreover, the same structural and functional parameters were assessed on mice reloaded for 6 days following 2 weeks of hindlimb unloading, in order to study the effects of the return to normal mechanical stress.

2 | MATERIALS AND METHODS

2.1 | Animals

Fifty-four male C57BL/6J mice, 14 weeks old, were used in the experiment. They were housed singly in cages in temperature-controlled rooms (22°C) under a 12 h light–dark cycle. The animals were fed a standard diet ad libitum. This study was approved by the Committee on the Ethics of Animal Experiments of Languedoc Roussillon in accordance with the guidelines from the French National Research Council for the Care and Use of Laboratory Animals (CEEA-LR-14002). Every effort was made to prevent discomfort and suffering.

2.2 | Experimental procedures

Thirty-six mice were subjected to hindlimb unloading through tail suspension according to the hindlimb suspension protocol described by Amblard et al. (2003).[26] Eighteen suspended mice were sacrificed after 2 weeks (HU group). The remaining 18 suspended mice underwent ambulation recovery for 6 days (HUR group) and were then sacrificed. During recovery, these reloaded mice were housed in cages similar to those in which they were suspended. Mice in the control group (CTL, $n = 18$) moved freely in their cage. All mice were euthanized by cervical dislocation after sedation via isoflurane inhalation. The experimental design of the study is described in Figure 1.

2.3 | Muscle and ankle sampling

Thirty mice (26.5 g ±0.3) were assigned to biological studies (BLE, 10 mice from each group). Each animal's two hindlimbs were harvested and the legs were dissected immediately after sacrifice. The Achilles and plantaris tendons were cut to a 2 mm distance from the calcaneus. The right soleus muscles were rapidly dissected out for muscle atrophy assessment, individually

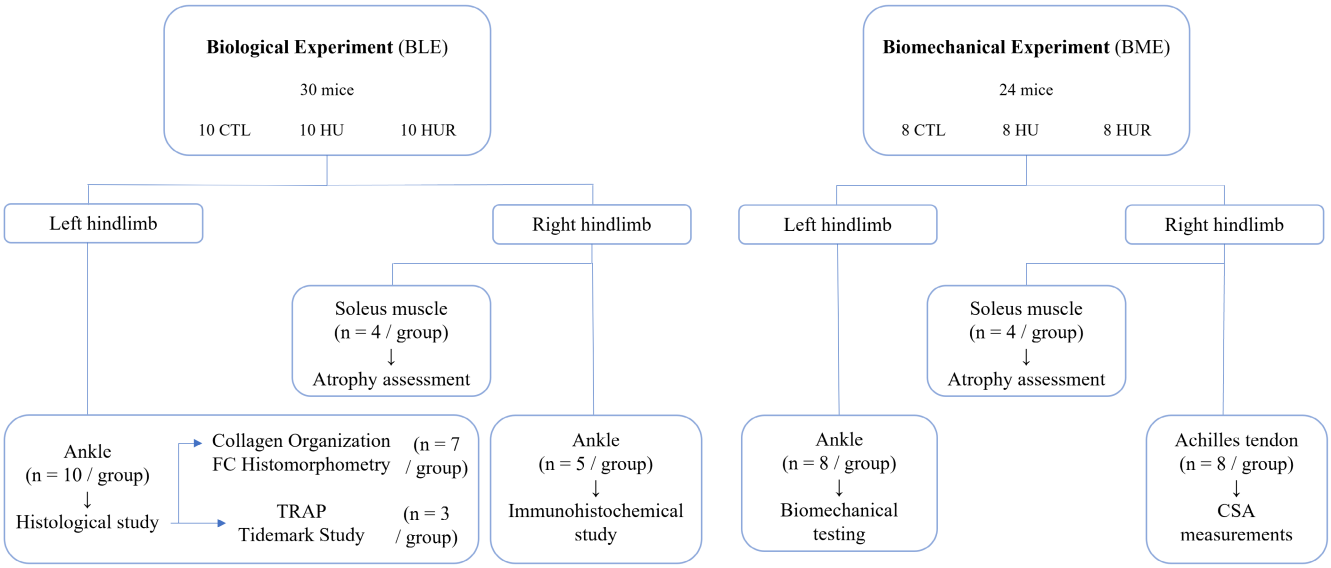

FIGURE 1 Experimental design of the study

weighed, immediately frozen in isopentane cooled with liquid nitrogen, and stored at −80°C. Then, both ankles, including the tibio-talus and the talo-calcaneal joints, were removed en bloc. Before sample fixation, the calcaneus was systematically positioned perpendicular to the tibia.

2.4 | Soleus muscle atrophy assessment

The degree of soleus muscle atrophy was assessed to validate the hindlimb unloading model. After weighing the muscle, transverse 10 µm thick sections of soleus were obtained at the mid-belly of the muscle using a cryostat (Leica© CM3050S, Wtzlar, Germany) and were subjected to laminin immunostaining for subsequent fiber cross-sectional area (CSA) measurements. The laminin immunostaining protocol is described in the "immunohistochemical study" section. Soleus CSA measurements were acquired using laminin images by hand-tracing single stained muscle fibers in ImageJ software. For four muscles in each group (CTL, HU, and HUR), we measured the CSA of 50 randomly selected muscle fibers. The average of these measurements was calculated for each muscle. Finally, the average CSA and average soleus muscle weight per group were calculated.

2.5 | Achilles tendon enthesis histological study

The left ankles of all mice from each group were fixed in 4% formaldehyde (Merk Millipore) in 0.01M phosphate buffer saline (PBS) (Sigma-Aldrich) at pH 7.4 for 1 week.

2.5.1 | Fibrocartilage histomorphometry and Collagen fiber organization

Seven left ankles from each group were embedded in paraffin for fibrocartilage histomorphometry and collagen fiber organization assessments. Following fixation, tissue samples were washed with deionized water, decalcified by 14% EDTA, dehydrated, cleared with Histoclear II (National diagnostics), and embedded in paraffin (Leica, Paraplast plus). To facilitate comparisons between groups, entheses were cut in the same orientation (sagittal plane) and sections were cut to a uniform thickness (8 µm). Sections of the Achilles tendon enthesis were obtained using a microtome (Leica© RM 2265, Wetzlar, Germany). For the fibrocartilage histomorphometry, two sections located in the median part of the enthesis were stained with toluidine blue (pH 3.7), dehydrated, and mounted with a resinous mounting medium (Entellan, Merk Millipore). Sections were stained with toluidine blue so that its metachromasia would identify fibrocartilage. This cationic metachromatic blue dye binds to the PG, staining the matrix purple-red.[21,27] Stained sections were imaged at a magnification of ×20 using a microscope (Olympus BX40) equipped with a CDD camera (Olympus, DP21). The area of uncalcified fibrocartilage (UFc) and the area of calcified fibrocartilage (CFc) of the Achilles enthesis were quantified using Image J software (2.0.0). Surface areas of UFc and CFc were manually delineated. The tidemark was used to delimit the distal boundary of UFc and the proximal boundary of CFc. The area of metachromasia above the tidemark defined the area of UFc (Figure 2A). To distinguish the CFc of the Achilles enthesis from that of the plantar fascia enthesis, stained sections were also analyzed under polarized light. The latter allowed us to clearly distinguish the end of CFc

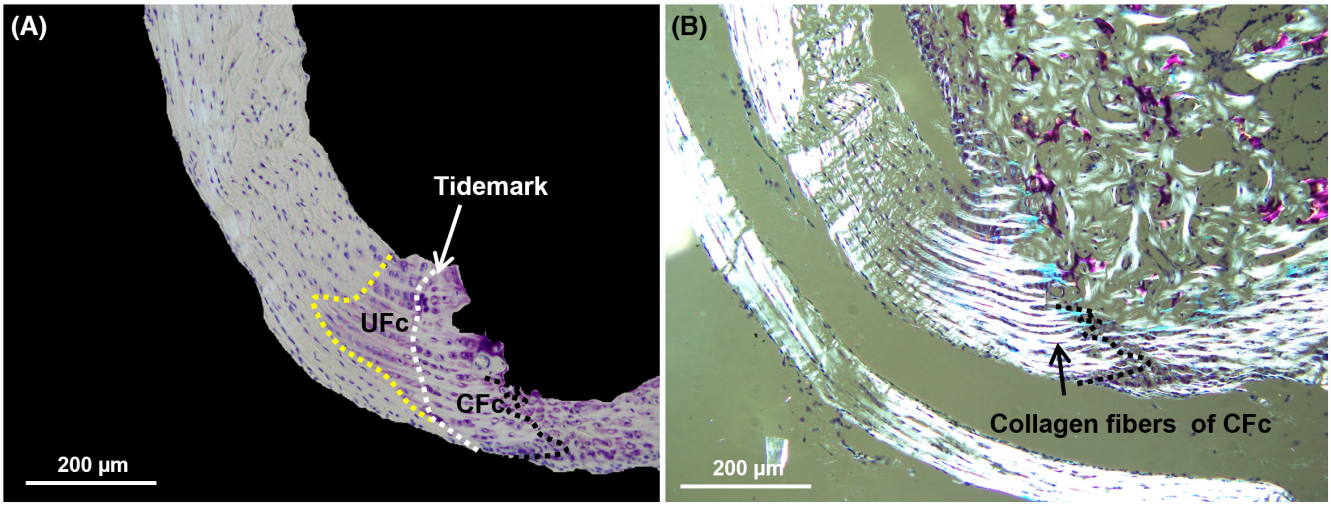

FIGURE 2 Delineation of UFc and CFc. Toluidine blue staining of the Achilles tendon enthesis viewed under transmitted (A) and polarized light (B). Areas of metachromasia above the tidemark (between the yellow and white dotted lines) define the UFc surface area (A). CFc is delineated by the tidemark in the proximal zone and by the osteochondral interface in the distal part. The latter can be clearly observed under polarized light (black dotted line) (B).

collagen fibers of the Achilles enthesis and then delineate the distal boundary of CFc (Figure 2B). In the HUR group, as two tidemarks were systematically observed, the tidemark closest to the tendon was always taken into account. For each histomorphometric parameter (UFc, CFc), the measured values from the two selected sections per sample were averaged and statistical analysis was performed on these average values.

For the collagen fiber organization study, the sections located in the median part of the enthesis were stained with Picrosirius red according to the method described by Junqueira et al. (1979)[28] and with toluidine blue (pH 5). They were viewed under polarized light to assess collagen fiber organization. All sections were observed in the same orientation. They were positioned under the microscope so that the collagen bundles which cross the tidemark at its median part were horizontal.

2.5.2 | Tidemark study and TRAP staining

Three left ankles from each group were embedded in methylmethacrylate resin (MMA) for tartrate-resistant acid phosphatase (TRAP) staining and to study the tidemark. Following fixation, tissue samples were washed with deionized water and dehydrated through an ethanol gradient of 60%, 80%, 95%, and 100% ethanol, each step lasting 48 h. Samples were cleared in methylcyclohexane (VWR international) for 48 h, infiltrated, and embedded in MMA resin (VWR international). They underwent polymerization in a 32°C water bath for 3 days. After block trimming, 5 µm-thick sagittal sections of the Achilles tendon enthesis were obtained using a microtome equipped with a D-profile tungsten-carbide knife. The sections were transferred to Superfrost Plus slides and stretched with 70% ethanol. The slides were covered with a plastic film, pressed, and dried for 2 days. TRAP staining and the tidemark study were realized on sections located in the median part of the enthesis. Before staining, MMA was removed from the sections by immersion in three changes of 2-methoxyethylacetate (Merk Millipore) for 20 min each, one change of ethanol 70% for 5 min, one change of ethanol 40% for 5 min, and then rehydrated in two deionized water baths.

TRAP is an enzyme found mainly in osteoclasts and is currently used for the assessment of bone resorption.[29,30] Rehydrated sections were incubated at 37°C overnight in a substrate solution consisting of 1 ml naphthol AS-TR phosphate substrate mix (15 mg Naphthol AS-TR Phosphate dissolved in 1 ml N,N dimethylformamide) in 100 ml acetate buffer (pH 5.0) enriched with sodium tartrate. The slides were then transferred without rinsing to a revelation solution consisting of 1 ml sodium nitrite (4% in distilled water), 1 ml pararosaniline dye, and 100 ml acetate buffer (pH 5.0) enriched with sodium tartrate and incubated for 10 min at 37°C. The sections were rinsed in water for 5 min and counterstained with toluidine blue (pH 5.0). They were dehydrated and mounted with entellan. Control sections were incubated in a solution not containing the substrate. No staining developed in these control sections.

For the tidemark study, sections were first stained with toluidine blue (pH 5), temporarily mounted with ethanol, and examined under a light microscope equipped with a CCD camera. Photographs of the Achilles tendon enthesis were taken under a 40× objective. The same

sections were then stained with Von Kossa, dehydrated, and mounted with entellan. Photographs of the Achilles tendon enthesis were taken again under the same objective. With the toluidine blue and Von Kossa stainings highlighting, respectively, tidemarks and mineralization fronts, photographs of sections from the same enthesis stained with the two dyes were overlaid via Adobe Photoshop 6.0 software. This enabled us to determine the position of the tidemark in relation to the mineralization front.

2.5.3 | Immunohistochemical study

For collagen II (coll II) immunostaining at the enthesis, the right ankles of each group were fixed for 48 h in 70% ethanol at 4°C, washed in PBS (0.01M, pH 7.4), and decalcified in 14% EDTA for 3–4 days. Samples were infiltrated for 24 h with PBS containing 10% sucrose, embedded in tissue-freezing medium (Leica), and frozen in isopentane cooled with liquid nitrogen. Eight micrometer-thick sagittal sections of the Achilles tendon enthesis were obtained using a cryostat and placed onto Superfrost Plus slides. Sections were air-dried, rehydrated, and digested for 3 h with testicular hyaluronidase (1 mg/mL in PBS, pH 5.0) at 37°C. They were submerged in 0.3% hydrogen peroxide solution for 30 min to quench endogenous peroxidase activity. They were blocked with Vector Labs mouse Ig blocking reagent and subsequently with a diluted solution of protein concentrate stock solution (M.O.M diluent) according to the supplier instructions of Vector labs Mouse on Mouse immunodetection Kit (BMK-2202). Sections were incubated with primary antibody against coll II (Invitrogen, MA5-13026, mouse monoclonal antibody, 1/50 in M.O.M diluent) for 30 min at room temperature. After rinsing with PBS, sections were incubated with biotinylated secondary antibody (M.O.M kit, 1/250 in M.O.M diluent) for 10 min at room temperature, rinsed, and incubated with an avidin-biotin complex conjugated to horseradish peroxidase (Vector Labs, Vectastain elite ABC kit) for 30 min at room temperature. Diaminobenzidine (DAB, Sigma) was used as the chromogen. Sections were dehydrated and mounted with entellan. Coll II immunostaining was performed on 5 samples from each group.

For laminin immunostaining on the soleus muscle, sections were air-dried, rehydrated, and treated with horse serum (1/10 diluted with BSA 5%). Then they were incubated with primary antibodies for laminin (Sigma L9393, rabbit polyclonal antibody, 1/30) for 2 h. As with the coll II immunostaining, the first antibody was detected using a biotin-conjugated secondary antibody (Vector, BA-1100, 1/100, incubation time: 1 h) with the Vectastain elite ABC peroxidase kit. For each antibody, control sections with only the secondary antibody deposited were prepared. No specific immunostaining was developed in these control sections.

2.6 | Biomechanical testing

Twenty-four mice (21.6 g ± 0.6) were used for the biomechanical study (BME, eight from each group). Uniaxial tensile tests were performed on 8 mice from CTL, HU, and HUR groups in order to determine the mechanical properties of the Achilles tendon enthesis. Each animal's left leg was dissected in such a way as to retain only the foot, Achilles tendon, and triceps surae. During dissection, the tendon of the plantaris was removed and the tibia was cut at its distal extremity. The samples were preserved at −80°C until the tensile test. On the right leg of each animal, the Achilles tendon was cut proximally at the myotendinous junction and distally about 2 mm above the Achilles enthesis. Samples were fixed for 48 h in 70°C alcohol and then cryoprotected in 10% sucrose solution (buffered in PBS) overnight before being cryofixed in isopentane pre-cooled in liquid nitrogen. The right soleus muscles were dissected out for muscle atrophy assessment, weighed, immediately frozen in isopentane pre-cooled with liquid nitrogen, and stored at −80°C.

2.6.1 | Soleus muscle atrophy and Tendon CSA

Soleus muscle atrophy was assessed on this BME series of animals ($n = 4$) according to the procedure described above (see soleus muscle atrophy assessment). For Achilles tendon CSA measurements, transverse 10 µm-thick sections were collected every 200 µm along the entire length of the tendon using a cryostat and were stained with eosin. Achilles tendon CSA measurements were acquired using eosin-stained images in ImageJ software (×10 magnification). CSA measurements were averaged for each tendon. Then the average per group was calculated ($n = 8$ for each group).

2.6.2 | Uniaxial tensile test

After thawing, the foot was attached with Prolene© 2/0 sutures to pre-cut support designed so that the angle between the foot and the Achilles tendon was 135°. This angle allows tensile strength to be applied in a

TABLE 1 Muscle mass and myofiber CSA of the soleus in biological and biomechanical experiments

	BLE			BME		
	CTL	HU	HUR	CTL	HU	HUR
Soleus muscle mass (mg)	8.00 (±.96)	5.61 (±.67)[†,‡]	7.6 (±.86)	5.76 (±.87)	3.21 (±.37)[†,‡]	6.19 (±.63)
Soleus myofiber CSA (μm^2)	1506 (±546)	934 (±329)[†]	982 (±354)[†]	1071 (±185)	626 (±50)[†,‡]	781(±20)[†]

[†]Significantly different from CTL.

[‡]Significantly different from HUR ($p < .05$).

physiological axis to the murine tendon.[31] The muscle fibers of the soleus and gastrocnemius were carefully stripped with a scalpel to expose the tendon layers. Then the Achilles tendon was gripped with a 12 cm Mayo-Hegar needle holder as close as possible to the enthesis. The support fixed to the foot and the Mayo-Hegar needle holder clamped to the Achilles tendon were positioned, respectively, in the lower and upper grips of the Instron 5566A universal testing machine fitted with a 100 N load cell (accuracy $\pm 5 * 10^{-4}$ N). Testing to failure was conducted at a speed of 2 mm/min. During the test, the sample was hydrated regularly with PBS. Strength as a function of displacement was recorded during the test using BlueHill 3 software. At the same time, local displacement of the enthesis was recorded with a Veho camera driven by Micro Capture Software. Maximum strength was determined from the load-displacement curves and corresponded to the load at failure for every sample tested. When the sample was in the elastic domain, a time range was determined from the load-displacement curves and reported on the video recording. A virtual point of interest was placed on the video at the distal part of the enthesis and the local displacement of the enthesis was determined in this time range by tracking the point displacement using Kinovea software. The local stiffness of the enthesis was then calculated as the ratio between the variation of the load and the variation of the local displacement during this same time range. To determine the site of failure histologically, after testing, each sample was prepared for paraffin embedding according to the method described above. Seven micrometer-thick sagittal sections spaced 50 µm apart across the thickness of the enthesis were obtained. The sections were stained with toluidin blue (pH 5), dehydrated, and mounted with entellan.

2.7 | Statistical analysis

Due to the small size of the groups, nonparametric tests were used. The nonparametric Kruskal-Wallis test was used to compare the measured parameters (UFc area, CFc area, soleus muscle weight, soleus muscle CSA, Achilles tendon CSA, Achilles Tendon enthesis strength and stiffness) between the three groups (CTL, HU, HUR). Multiple comparisons were made via the Conover-Iman test with a Bonferroni correction. Statistical analysis was performed using XLSTAT software. The significance level was set at $p < .05$.

3 | RESULTS

3.1 | Severe atrophy of the soleus muscle after 14 days of unloading and partial recovery with reloading

For the BLE and BME experiments, statistical analysis revealed a statistically significant inter-group difference (Table 1) in soleus weight ($p < .001$ for BLE and BME) and muscle fiber CSA ($p < .01$ for BLE and BME).

Soleus weight changed significantly after 14 days of suspension compared to CTL, decreasing by approximately 30% and 44% ($p < .001$) in the BLE and BME experiments, respectively. The CSA of muscle fibers also decreased significantly in HU compared with CTL, by about 38% and 41.5% ($p < .001$) in BLE and BME, respectively. After 6 days of reloading following HU, no difference in soleus muscle mass compared to CTL mice was observed in the two sets of experiments. However, the mean CSA of soleus fibers was not restored in either BLE or BME ($p < .003$).

3.2 | UFc but not CFc areas were reduced by unloading while reloading increased both

The Achilles tendon entheses of the CTL group (Figure 3A) showed the four zones classically described in a fibrocartilaginous enthesis: tendon, fibrocartilage, calcified fibrocartilage, and bone. Calcified and uncalcified fibrocartilage were separated by the tidemark. The fibrocartilage consisted of cells surrounded by an intense metachromatic pericellular matrix arranged in a columnar pattern

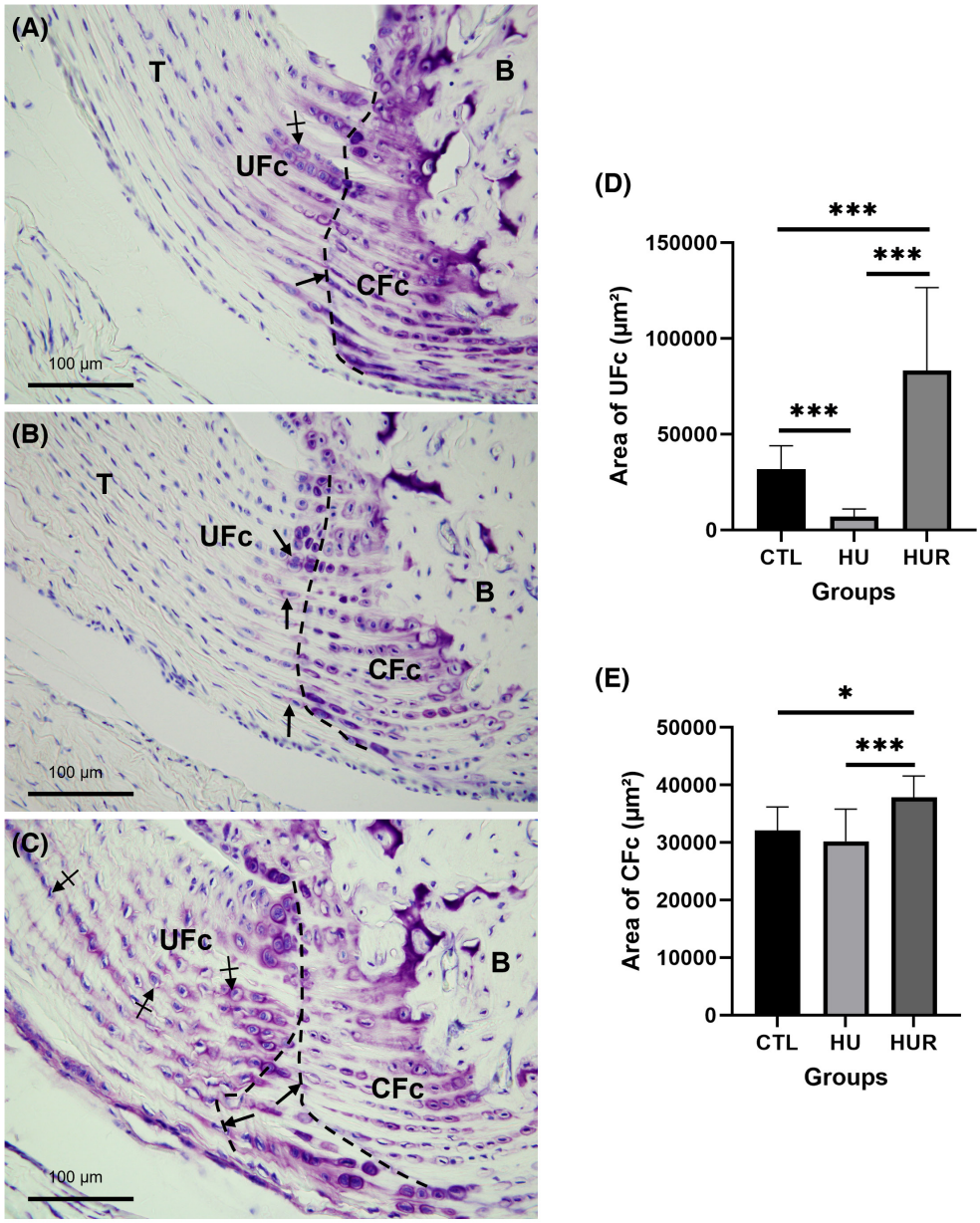

FIGURE 3 Toluidine blue-stained sections of CTL (A), HU (B), and HUR (C) groups and areas (μm^2) of UFc (D) and CFc (E). In the CTL group, UFc and CFc are clearly identifiable between the tendon (T) and the bone (B). They are separated by the tidemark (arrow). The rounded cells are organized in columns and separated by collagen fibers. They have a pericellular matrix rich in proteoglycans (cross arrow). In the HU group, very little metachromasia is observed in the extracellular matrix of the UFc. Only the pericellular matrix of cells close to the tidemark shows the expression of proteoglycans (arrows). In the HUR group, numerous round cells with a metachromatic pericellular matrix (cross arrows) are found relatively far from the tidemark. Two tidemarks are present in the superficial part of the enthesis (arrows). Significant inter-group difference (*$p < .05$; ***$p < .001$). All values are means. Error bars designate the standard deviation.

alternating with collagen fibers and perpendicular to the tidemark. After a 14-day suspension (Figure 3B), only the calcified fibrocartilage was clearly identifiable. The boundary between tendon zone and uncalcified fibrocartilage was difficult to distinguish because of the very weak extracellular matrix metachromasia. Although the cells were always aligned, only the cells adjacent to the tidemark had a pericellular matrix expressing proteoglycans. In the HUR group (Figure 3C), the four zones of the enthesis were again clearly distinguishable due to the intense metachromatic extracellular matrix of the UFc. In addition, there were many round cells with a metachromatic pericellular matrix situated relatively far from the tidemark which, in most cases, was double.

Comparing the three experimental groups, we found a significant difference in both UFc area ($p < .001$) and CFc area ($p = .025$). Concerning UFc (Figure 3D), the multiple comparisons showed that HU mice had a significantly

different UFc area from both the CTL group ($p = .005$) and the HUR group ($p = .005$). Fourteen days of hindlimb suspension led to a 78% decrease in UFc area compared with CTL animals, whereas the UFc area of HUR mice increased 12-fold compared to the HU group. Moreover, the HUR UFc area was significantly different from that of CTL ($p < .001$). The area of UFc metachromasia was twice as high in HUR as in CTL. Concerning CFc (Figure 3E), no difference was observed between the CTL and HU groups. However, the multiple comparisons showed that HUR mice had a significantly different CFc area from both CTL ($p = .036$) and HU ($p = .006$). Reloading the mice led to a 25% increase in CFc area compared with HU animals. In addition, the area of CFc metachromasia in reloaded mice was 15% higher than that of CTL animals.

3.3 | No effect of loading on resorption at the Achilles tendon enthesis

Although many osteoclasts were observed in the tibia and calcaneus in HU and HUR groups compared to CTL (Figure 4B,C, inserts), no osteoclast was detected either at the tidemark or at the enthesis osteochondral junction in any of the groups (Figure 4).

3.4 | Progression of mineralization front in the direction of the tendon with reloading

Unlike the CTL and HU animals, where only one tidemark forming a straight line separating the UFc from the CFc was observed, the HUR group consistently showed two tidemarks in the bottom half of the enthesis. When the undecalcified resin sections were sequentially stained with toluidine blue (Figure 5A) and then Von Kossa (Figure 5B), two tidemarks were observed after the toluidine blue and only one tidemark after the Von Kossa staining. This indicates that reloading led to a progression of the mineralization front toward the tendon, resulting in the appearance of a mineral protuberance in the superficial part of the enthesis and thus breaking the rectilinear course of the tidemark.

3.5 | Unloading and reloading alter collagen fiber organization only in the UFc

In the CTL group, the entheseal fibrocartilage showed dense collagen bundles, homogeneous in thickness, parallel to each other, and separated by rows of chondrocytes (Figure 6A). The organization of collagen fibers in the CFc was not affected by either unloading or reloading. In contrast, changes in collagen fiber organization were observed in the UFc. In HU (Figure 5B), a loss of parallelism of collagen bundles was observed, and collagen bundle thickness was heterogeneous. Collagen bundles were thinner in the superficial part of the enthesis and there were more interfibrillar spaces. Within the bundles, the fibers were less densely packed than in controls. In the HUR group (Figure 6C,D), a strong decrease in collagen birefringence was observed compared with the other groups. When HUR sections were observed from a different polarization angle, the continuous collagen bundles appeared to have lost their alignment and were highly crimped (Figure 6D) compared to CTL and HU.

3.6 | Unloading and reloading affected the distribution of collagen II expression in the enthesis UFc

Differences in the distribution of coll II expression were found only in UFc (Figure 7). In the UFc of the CTL animals, coll II was expressed at the periphery of most cells

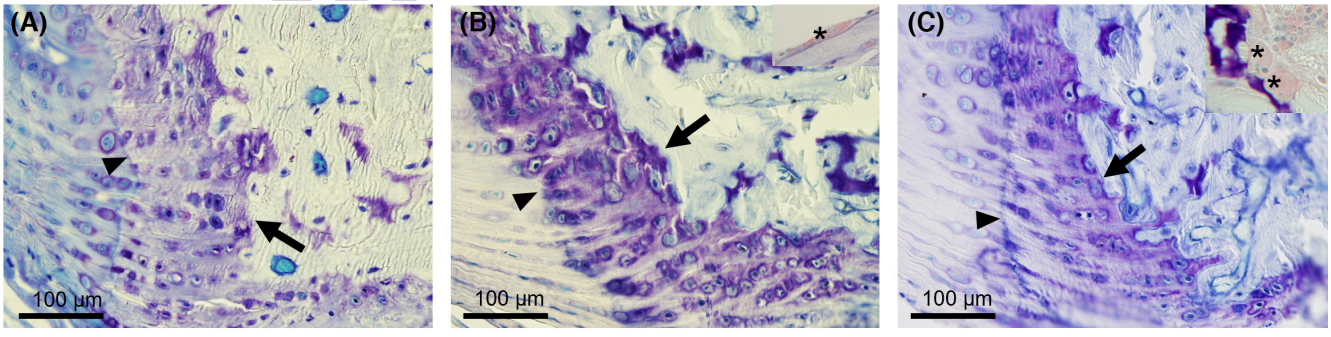

FIGURE 4 TRAP activity in CTL (A), HU (B), and HUR (C) mice at both Achilles tendon enthesis and bone. At the enthesis, no TRAP-positive cells were observed either at the tidemark (arrowheads) or the osteochondral junction (long arrows) in any group. In contrast, TRAP-positive cells (asterisks) were repeatedly observed in the tibia and calcaneum of HU and HUR animals (B, C inserts).

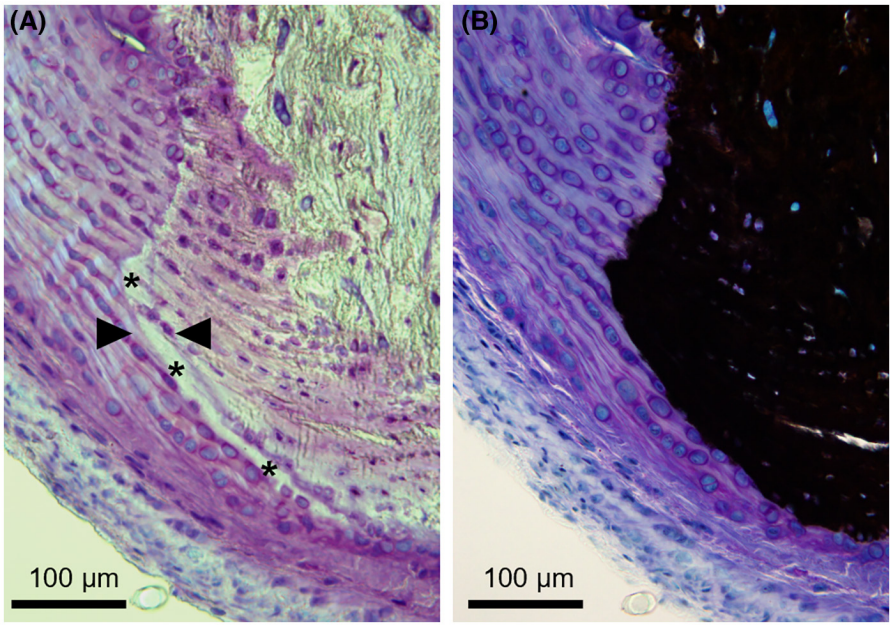

FIGURE 5 Photographs of a single undemineralized section of HUR Achilles tendon enthesis stained successively with toluidine blue (A) and Von Kossa (B). Two tidemarks (arrowheads) are observed in the superficial part of the enthesis after toluidine blue staining while no tidemark appears in front of the mineralization front after Von Kossa staining. Note that the mineral protuberance (asterisks) between the two tidemarks is poorly metachromatic.

in the medial and superficial areas of the fibrocartilage, from the tidemark to a virtual line in the mid-calcaneal part of the tendon (Figure 7A). Located at the periphery of the chondroplasts, the coll II immunostaining extended into the adjacent matrix, where coll II deposits formed bands oriented in the direction of the collagen fibers. In the HU group, no immunoreactivity was observed in the superficial zone of the UFc, in contrast to the UFc medial zone (Figure 7B). In the HUR group, a larger area of coll II immunoreactivity was observed than in CTL and HU (Figure 7C). This area extended into the tendon as far as the calcaneal tuberosity. As in the CTL group, the periphery of chondroplasts located in the superficial and medial zones of the fibrocartilage was immunopositive. Within the CFc, no significant difference was observed between groups, with coll II expressed throughout the extracellular matrix as well as in the periphery of the chondroplasts.

3.7 | While unloading modified site of failure of the tendon-enthesis-bone unit and reduced enthesis stiffness, reloading restored enthesis elastic properties

Although no difference in tendon CSA was found between the CTL, HU, and HUR groups (Figure 8C), there were significant changes in the structural properties of the tendon-enthesis-bone unit after unloading (Figure 8). Compared to the CTL samples, the mean values for maximum load at failure of the HU samples increased significantly by 25% ($p = .0271$) (Figure 8A). In addition, local stiffness at the enthesis was significantly reduced by 35% after the 14 days of suspension ($p = .001$) (Figure 8B). Investigations of the effect of reloading revealed a significant difference in stiffness between HU and HUR ($p < .001$). While HUR enthesis stiffness increased by 66% compared to HU, it did not differ significantly from CTL (Figure 8B). In addition, no difference in maximum load at failure was observed between HUR and CTL (Figure 8A). The histological study of the failure site revealed inter-group differences in sites of failure during the tensile test (Figure 8D,E). In the CTL and HUR groups, failure occurred predominantly at the enthesis, more precisely at the osteochondral junction (Figure 8E). In the HU group, only one specimen failed at the enthesis. Seventy-five percent of failures occurred at the bone, more precisely near the posterior side of the calcaneum below the enthesis (Figure 8E). In addition, the failure profiles of all samples showed a fragile-type failure with elastic behavior before breaking (Figure 8F).

4 | DISCUSSION

The musculoskeletal system adapts not only to environmental changes like altered microgravity but also to chronic reduction of earthly mechanical constraints like a sedentary lifestyle, clinical bed rest, or joint immobilization. While muscle and bone adaptations to deconditioning have been widely described, few studies have focused on the specific junction site between tendon and bone, i.e., the enthesis. The purpose of our study was to examine and clarify the effects of mouse hindlimb unloading and reloading specifically on the Achilles tendon enthesis. Our hypothesis was that chronic changes in mechanical stress would affect fibrocartilage quantity and composition, leading to mechanical weakness of the enthesis. This hypothesis was partially validated: while the

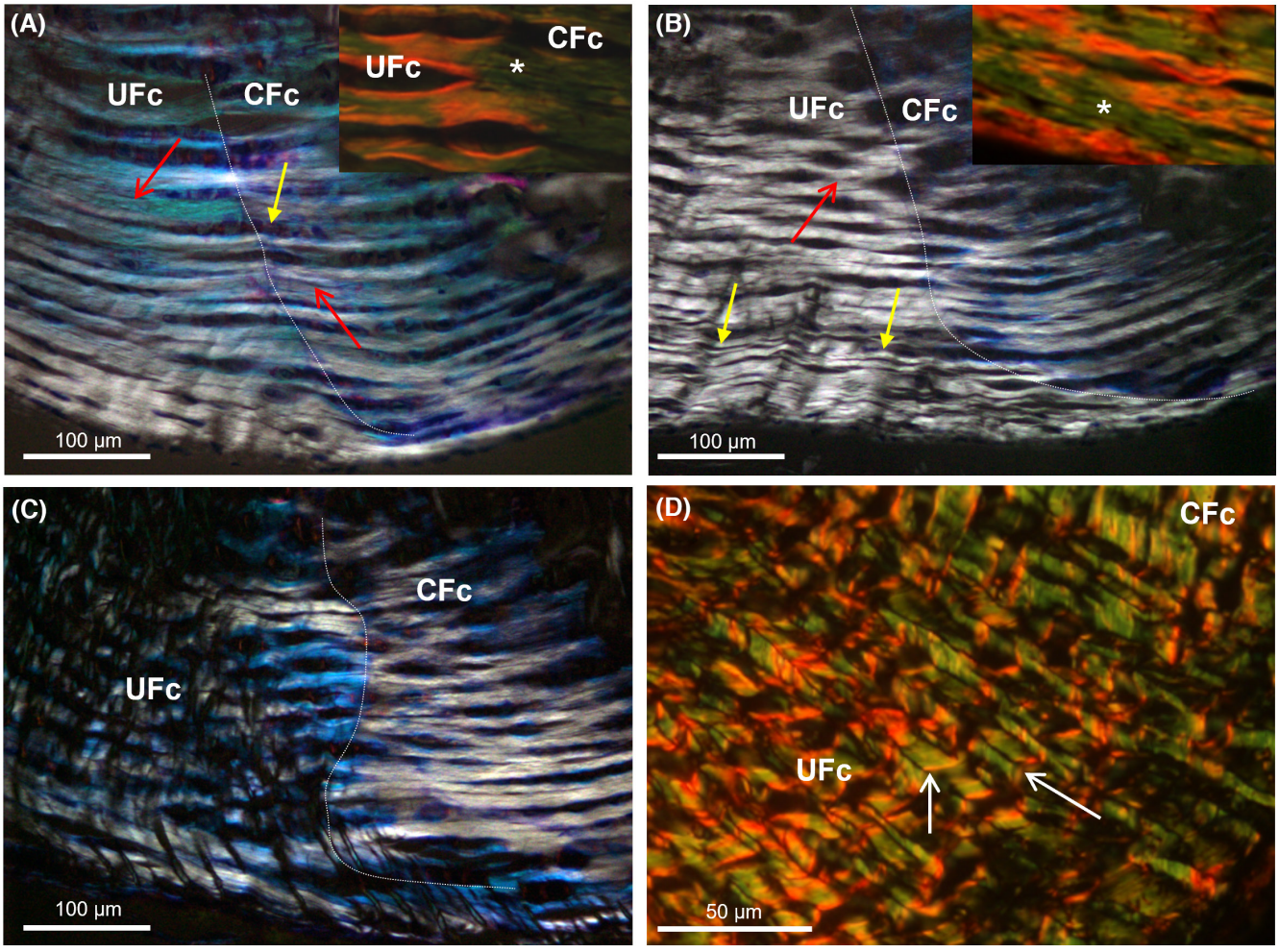

FIGURE 6 Toluidine blue- (A, B, C) and Picrosirius red- (A inlay, B inlay, and D) stained sections viewed under polarized light in CTL, HU, and HUR groups. Alternating parallel rows of cells (yellow arrow) and uniformly-sized collagen bundles (red arrows) can be observed in the enthesis fibrocartilage of the CTL animals. Within the bundles, the fibers are densely packed (A insert). In the HU group, loss of parallelism of collagen bundles (red arrow) is observed in the UFc and thinner collagen bundles are found in the superficial part of the enthesis (yellow arrows). Within the bundles, there are more interfibrillar spaces (asterisk) compared to CTL (B insert). In the HUR group, with the same orientation of the enthesis under the microscope, low birefringence is observed in the UFc (C). When sections are observed from a different polarization angle, the continuous collagen bundles appear highly crimped (white arrows, D).

enthesis structure changed in response to unloading and reloading, altered mechanical stress impacted the elastic properties and modified the site of failure of the tendon-enthesis-bone unit.

To unload the Achilles tendon enthesis, we chose the hindlimb-unloading rodent model,[25] commonly used to simulate weightlessness. This model induces many physiological changes that are similar to those experienced by astronauts during space flight, including a cephalic fluid shift and loss of water volume as well as diminished bone and muscle mass.[26,32] After 14 days of suspension, soleus muscle mass and fiber mean CSA was strongly reduced in our two sets of experiments (biological and biomechanical experiments) compared with CTL. Our results are in agreement with the literature, where major atrophy was observed in the soleus, a postural muscle, following 14 days of hindlimb unloading.[32] The latter study also described a 24.5% decrease in the mean CSA of gastrocnemius slow fibers, a 41% decrease in the normalized peak tetanic response of the soleus, and more broadly, a 25% decrease in hindlimb force. In view of these data, the severe atrophy of the soleus we observed strongly suggests that the load transmitted to the Achilles tendon by the soleus and gastrocnemius muscles is reduced after 14 days of suspension. In addition, with the mice no longer supporting their body weight, the compressive stress normally applied at the enthesis during foot dorsiflexion[33] should be reduced by hindlimb suspension.

Although our study is the first to describe the fibrocartilage response in the Achilles tendon enthesis under unloading conditions, previous studies reported fibrocartilage remodeling linked to hypoactivity in other entheses

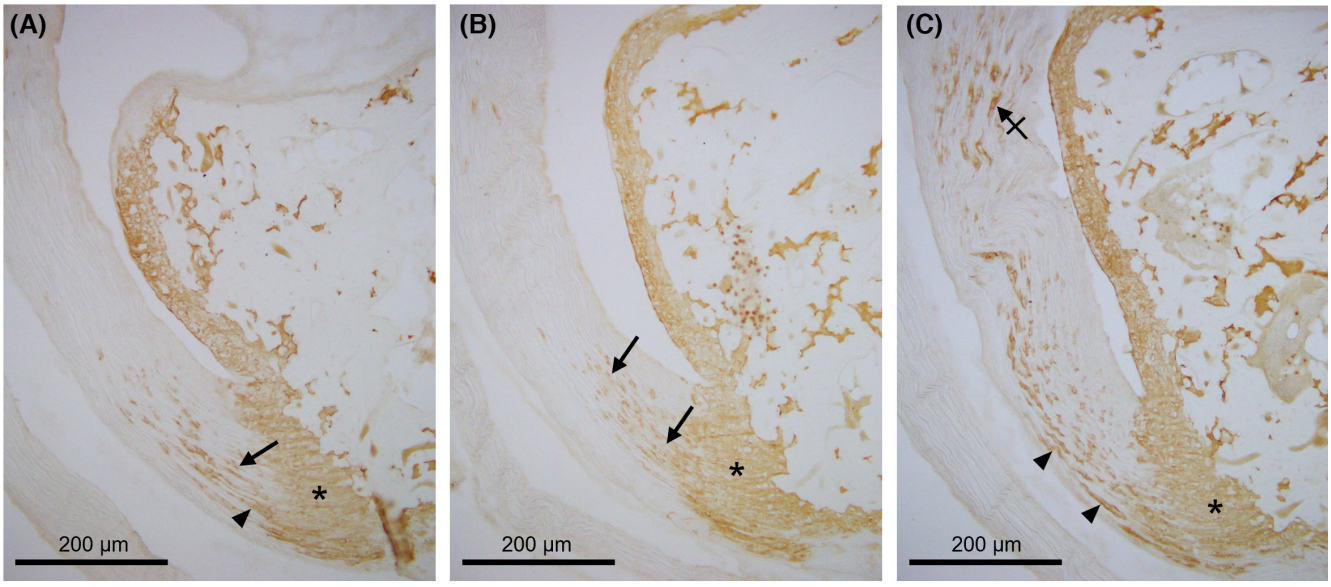

FIGURE 7 Coll II expression in the Achilles tendon enthesis in the CTL (A), HU (B), et HUR (C) groups. No inter-group difference was found in the expression of coll II in the CFc (*). In the CTL group, coll II expression was observed in the medial (long arrow) and the superficial (arrowhead) parts of the enthesis UFc. In contrast, the HU group only showed coll II immunolabeling in the medial part of the enthesis (long arrows). In the HUR group, coll II expression was restored in the superficial part of the enthesis UFc (arrowheads), extending into the tendon as far as the calcaneal tuberosity (cross-arrow).

of the lower limb, including the bone-tendon attachment of the rat quadriceps muscle[21,22] and the patellar tendon insertion.[23] Performing their analysis on the entire fibrocartilaginous zone without distinguishing between UFc and CFc, Frizziero et al. (2011) and Mutsuzaki et al. (2015) described a decrease in the area of fibrocartilage and its PG content.[21,23] Our results, while consistent with these data, show that the loss of fibrocartilage under simulated microgravity conditions results from a decrease in UFc alone since CFc appeared to be very little affected by the reduction in mechanical load. In this mineralized part of the enthesis, we did not observe any difference between the CTL and HU groups in fibrocartilage surface area, coll II expression, and collagen fiber organization. Conversely, we found a 78% decrease in UFc surface area after 14 days of suspension compared to CTL. A decrease in UFc in response to unloading was also reported by[22] in the rat quadriceps tendon enthesis after 3 weeks of cast immobilization. The drastic decrease observed in UFc is indicative of a loss of PG, since Toluidine Blue, the cationic metachromatic blue dye that we used, is known to bind specifically to these macromolecules.[21,27] In addition to the loss of PG, we also observed a decrease in coll II expression particularly in the superficial zone of UFc, as well as moderate disorganization of collagen fibers. The latter, less densely packed and parallel to each other than in CTL, appeared thinner in the superficial part of the enthesis. Like other findings of collagen fiber disorganization in unloading conditions,[21–22,34] our results highlight the importance of mechanical stress in maintaining the integrity of collagenous structures of enthesis UFc. The changes in the UFc matrix in HU animals seem to stem from a reduction in the metabolic activity of the fibrocartilage cells, as suggested by the lack of PG deposits around the chondroplasts compared to CTL animals. A decrease in the number of fibrocartilage cells could also be involved since a decrease in the number and proliferation of chondrocytes in addition to an increase in the chondrocyte apoptosis rate have been reported under unloading conditions.[22,23]

Taken together, our results show that enthesis UFc tends to lose its fibrocartilaginous characteristics in an environment where the mechanical load is reduced. The lower compressive stresses induced by weightlessness probably explain this adaptation. The relationship between compressive stress and fibrocartilage tissues has already been demonstrated at the enthesis[12] and in other fibrocartilaginous structures such as menisci or intervertebral discs. In the Achilles tendon enthesis, where UFc is thicker in the area near the bursa, the greater compressive strain was described in the deep region than in the superficial region, due to tendon compression against the calcaneus during ankle dorsiflexion.[33] The higher the compressive stress, the thicker the UFc.[35,36] At a molecular level, the entheses are enriched in type II collagen as well as in PG and glycosaminoglycans such as aggrecan and hyaluronic acid, which have a high water-binding capacity[11,37,38] and which are believed to be involved in the

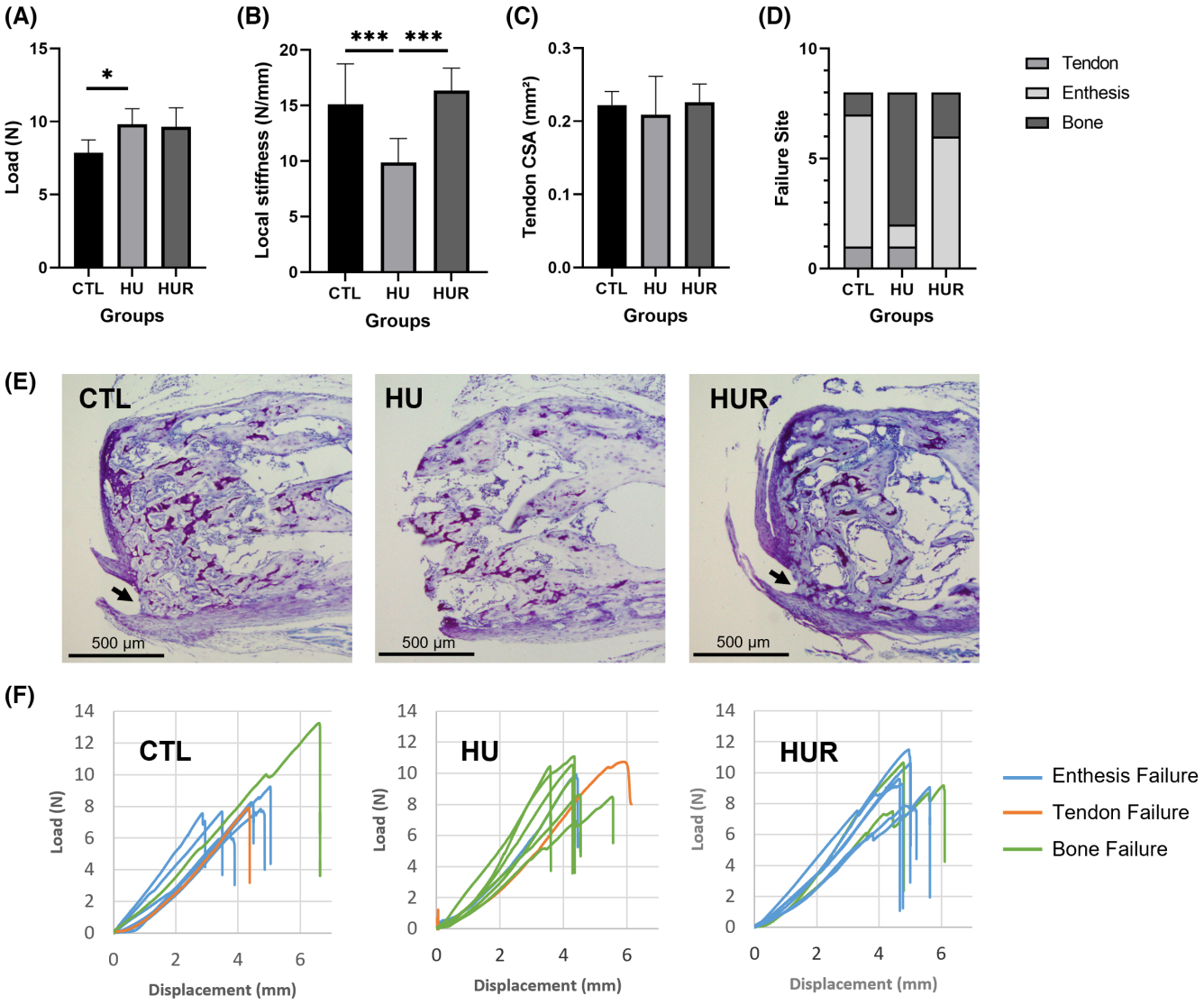

FIGURE 8 Maximum load at failure (A) (*$p < .05$), enthesis local stiffness (B) (***$p \leq .001$), and mean tendon CSA (C). Proportions of failure site induced by the tensile test (D). Toluidine Blue-stained sections of the main failure sites in each condition (E). Load–displacement curves of all samples for each condition (F). In CTL and HUR groups, failure occurred mainly at the osteochondral junction of the enthesis (arrows). Only a few deep and superficial tendon bundles remained attached to the bone. Note that the HUR group shows cortical partial restoration at the enthesis. In the HU group, open marrow spaces indicate bone failure in the posterior part of the calcaneus.

tendon's capacity to withstand compressive strength.[39,40] In menisci or intervertebral discs where compressive stress is high,[41] studies consistently reported a significant decrease in PG content in response to actual and simulated microgravity conditions.[42–44] Thus, the loss of enthesis fibrocartilaginous characteristics in the HU animals observed here is likely an adaptation to the change in the mechanical environment.

To determine whether unloading-induced fibrocartilage remodeling could impact the mechanical properties of the Achilles tendon enthesis, thereby weakening this interface, we performed a tensile test on the Achilles tendon-bone complex. While we expected reduced enthesis resistance to tensile stress after 14 days of suspension compared to CTL, we observed a significant increase in mean maximum failure strength in the HU group compared to CTL. The HU group value was consistent with the maximum failure strength reported for other mature mice entheses.[18,20,45] The difference in maximum failure strength was not related to a change in tendon size, since no difference in tendon cross-sectional areas was observed between the CTL and HU groups. In addition, the two groups' low variability of maximum failure strength values (<15%) and homogeneity of brittle failure profiles testify to the reproducibility of our protocol, ruling out methodological bias as an explanation for the difference observed between the two groups. Input from the histological study of the failure site helped us interpret this unexpected

result. This study revealed that, whereas the rupture occurred predominantly at the enthesis in the CTL group, in the HU group it consistently occurred in the bone near the posterior side of the calcaneus below the enthesis. The adverse effects of the microgravity environment on weight-bearing bones are widely documented.[1,3,4,46] The calcaneus, which is a largely trabecular bone, is no exception. We observed many more osteoclasts in the tibia and calcaneus in HU groups than in CTL, indicating increased resorption activity within these bones. The calcaneus is a suitable skeletal site for monitoring bone mineral loss and bone quality deterioration in weightlessness because it is representative of changes at other skeletal sites such as the vertebra and the femoral neck.[47] Assessing the bone microarchitecture of the calcaneus by microtomography, Deymier et al. (2020)[6] and Gerbaix et al. (2018)[48] studied the effects of spaceflight on the calcaneus. Deymier et al. (2020)[6] showed a trend toward decreased cortical thickness in the midsection of the mouse calcaneus after a 15-day spaceflight, without observing changes in either BV/TV or trabecular morphometry. On the contrary, Gerbaix et al. (2018)[48] reported a 6.4% decrease in whole calcaneus bone volume fraction without altered cortical thickness after 1 month of spaceflight compared to CTL. Very interestingly, however, this study also found that the volume of calcaneus bone loss was not homogeneous, being particularly marked at its proximal end where the Achilles tendon inserts. Similarly, if the proximal end of the calcaneus was particularly subject to bone erosion after 14 days of hindlimb suspension, this would explain why, during the tensile test, our samples failed within the bone and not at the osteochondral interface, despite enthesis remodeling. In a tensile test, the failure occurs where microstructural defects are observed,[49] and this also holds for composite materials.[50] Thus, in our study, the strain likely deviated to the weakest area of the sample, leading to failure within the bone. This observation is in line with the avulsion fractures described by Deymier et al. (2019) and Golman et al. (2021)[51] at the supraspinatus tendon insertion following monotonic uniaxial tensile loading in mice, where the supraspinatus muscle had been paralyzed by treatment with botulinum toxin. In the latter study, in contrast to our study, it has been reported a decreased maximum load in response to unloading, was positively correlated with a decrease in bone architectural parameters, such as trabecular and cortical thicknesses, BV/TV, or bone mineral density. However, it has been demonstrated that weightlessness led to altered bone elastic micromechanical properties independently of alterations in bone microarchitecture. Indeed, by performing an indentation study on vertebral bones (short bones such as the calcaneus), Gerbaix et al. (2017)[52] showed that 1 month of spaceflight resulted in a decrease in both hardness and elastic modulus without impacting the degree of bone mineralization. These alterations in micromechanical properties impact the material properties of the bone. The decrease in bone elastic properties at the micrometer scale makes the bone more deformable giving it similar properties to the material properties of the enthesis. The hypothesis we propose is that the enthesis-bone interface would become an interface between two materials whose micromechanical properties tend to look similar. This would solidify the interface and explains the increase in the maximum strength at failure in HU mice. Our hypothesis is only likely if changes in enthesis micromechanical properties are less important than changes in the bone material properties. Beyond this hypothesis, we cannot exclude the possibility that changes in the enthesis composition and/or structure may also explain our results. Further studies are needed to verify these assumptions.

While unloading modified the site of failure of the tendon-enthesis-bone unit, it also decreased enthesis stiffness: local stiffness at the enthesis was significantly reduced by 35% after a 14-days suspension compared to CTL. Several studies have investigated the effects of unloading on the elastic properties of the tendon-bone complex, with contrasting results. On the contrary, Schwartz et al. (2013)[34] and Matsumoto et al. (2003)[53] described a decrease in stiffness after both 4 and 8 weeks of unloading, respectively, in the mouse developing supraspinatus tendon enthesis under Botox[34] and in the rabbit immobilized Achilles tendon enthesis.[53] In contrast, in adult mice, the studies of Abraham et al., 2022 and Deymier et al. (2019; 2020) showed that supraspinatus tendon enthesis stiffness was unaffected by 3 weeks[20] or 4 weeks[18] of shoulder paralysis induced by botox injections, nor by 2- and 4-weeks spaceflights.[6] In this latter study, no spaceflight-induced change was observed in the stiffness of the Achilles tendon enthesis. It is difficult to compare our results with those of the literature since all these studies considered the tendon-bone complex, where a change in stiffness can be attributed to a change in the elastic behavior of the tendon body, enthesis, and/or bone. Here, seeking to determine the elastic behavior of the enthesis itself, we chose to calculate local enthesis stiffness based on a video recording of the local displacement of the enthesis during the tensile test. By so doing, we were able to identify a decrease in stiffness specifically affecting the enthesis.

We believe that the lower stiffness obtained for the HU mice could be related to the enthesis structural changes identified after the 14-day suspension. The mechanical behavior of connective tissue is governed both by the fibrous components and the ground substance of the tissue.[54,55] Since collagen fiber alignment has been shown to play a role in connective tissue tensile properties,[34] the disorganization in the UFc collagen fiber bundles (loss of

parallelism, varying thickness, less densely packed collagen fibers) in response to unloading could explain some of the reduced tensile stiffness we measured. However, in the mouse Botox-unloaded developing supraspinatus tendon enthesis, Schwartz et al. (2013)[34] suggested that the reduction in collagen fiber alignment accounted for only a small fraction of the reduced elastic modulus, and that compositional factors must also be involved. Both the degree of crosslinking in the collagen network and total collagen content have been shown to play a role in the determination of elastic properties of cartilage, fibrocartilage, and ligaments.[56] Although these biochemical parameters were not the focus of our study, we assessed PG content, which has been found to play a role in tendon stiffness.[54] Investigating the mechanical role of GAGs in tendons under tensile load, Rigozzi et al. (2009)[57] showed that partial removal of chondroitin sulfate and dermatan sulfate from the mouse Achilles tendon treated with chondroitinase ABC only induced a significant decrease in stiffness and elastic modulus in the distal region closest to the enthesis. In light of their findings, it is likely that PGs and GAGs are also responsible for the decrease in Achilles tendon enthesis stiffness in our HU animals since we observed a drastic decrease in PGs within the UFc extracellular matrix. Further research will be needed to determine how enthesis PGs and GAGs are involved in decreased stiffness. However, in view of the disorganization of collagen fibers in the UFc of the HU Achilles tendon enthesis, this may be related to the role some of them play in collagen fibril, fiber, and fascicle bridging.[54,58]

Understanding the changes that occur in muscle, tendon, and bone is an essential step toward limiting or preventing the deleterious effects of spaceflight. No less importantly, account must be taken of musculoskeletal structure responses when astronauts return to Earth, so as to optimize post-flight rehabilitation strategies. For this reason, we investigated the effects of 6-day reloading consecutive to the 14-day suspension period. During this recovery period, the mice were allowed to move freely in their cages. Our objective was to determine whether any remodeling of the enthesis induced by the simulated microgravity conditions could lead to an impairment of the enthesis structure when normal loading conditions resumed, potentially affecting its tensile mechanical properties.

Our histological study showed that the Achilles tendon enthesis response to reloading is adaptive. We did not observe any tears in the fibrocartilage, inflammatory or degenerative signs, or disunion at the osteochondral junction in HUR entheses. The very strong increase in PG content, as reflected by the more than 10-fold increase in UFc area in HUR mice compared to HU mice, in addition to the highest expression of coll II, all suggest an adaptation to re-exposure to compressive stress. Jarvinen et al. (1999)[22] demonstrated the capacity of the rat quadricipital tendon enthesis to retrieve its characteristics during the recovery period after 3 weeks of immobilization. These authors described a total recovery of enthesis fibrocartilage thickness with 8 weeks of low- or high-intensity treadmill running. However, our study indicates that enthesis recovery involves an early stage where fibrocartilage synthesis is exacerbated. The entheses of the HUR mice showed, after 6 days of reloading, overexpression of type II collagen, long rows of chondrocytes in the UFc, and greater UFc and CFc surface areas than CTL entheses. As no TRAP staining was observed at the osteochondral junction, the increase in CFc surface area does not seem to be related to the resorption of subchondral bone. It seems rather to be the result of a mineralization front progressing toward the tendon in the superficial part of the enthesis. Indeed, unlike CTL and HU mice, the HUR group showed two tidemarks, only one remaining visible with Von Kossa staining. The superficial region of the Achilles tendon enthesis is reported to display higher tensile strain during ankle dorsiflexion,[59] and the increase in surface area that we observed could therefore be a response to renewed tensile stress. Indeed, in addition to compressive stress, the reloading increased the loads applied externally via reaction forces or internally through muscle contractions, despite the incomplete muscle recovery it provided.

Although the enthesis was obviously undergoing structural remodeling after 6 days of reloading, the site of failure, maximum failure strength, and stiffness did not differ from CTL. Studies investigating bone recovery after reambulation report contrasting results. Whereas partial[60] or total recovery[61] of the BV/TV of the rodent tibia was observed after 14 days of reloading following 14 days of suspension, 8 days of earth reambulation worsened calcaneus bone loss induced by 1-month spaceflight.[48] However, in the latter study, there appeared to be a regional response: despite the significant decrease in cortical thickness compared with CTL, the thickness of the subchondral bone at the enthesis seemed to be partially restored within 8 days. This local response is probably linked to the return of tensile stress. Thomopoulos et al. (2007)[62] demonstrated the role of mechanical factors in supraspinatus tendon enthesis maturation during mouse post-natal development. These authors showed that reducing muscle load by chemically denervating the supraspinatus muscle with botulinum toxin A impeded accumulation of mineralized bone and prevented fibrocartilage accumulation at the enthesis. Our histological study findings are consistent with these previous results. Although osteoclasts were still present in the calcaneus after 6-day reloading, they were absent from the osteochondral junction. In addition, the

greater thickness of the subchondral bone at the enthesis compared to the HU animals indicates partial cortical restoration in response to the return of tensile stress, apparently sufficient to refocus the stress on the CFc-bone interface. Thus, in contrast to the HU mice, rupture occurred predominantly at the enthesis both in HUR and in CTL mice.

After the 6-day reloading, the elastic properties of the Achilles tendon enthesis were restored although the enthesis had not recovered the structural characteristics of CTL animals. As no difference in tendon CSA was found between the HU and HUR groups, the greater enthesis stiffness of the HUR animals was not due to changes in tendon dimensions but rather to local changes within the tissue. First, modified collagen fibers organization could explain the difference in stiffness between the two groups, in line with the study of Spiesz et al. (2018).[63] Comparing two functionally distinct equine tendons, these authors reported a correlation between collagen crimp angles and tendon stiffness. They showed that the superficial digital flexor tendon (an energy-storing tendon), which had collagen crimp angle smaller than the common digital extensor tendon (a positional tendon), had the highest stiffness. The high degree of UFc collagen fiber crimping that we observed in the HUR group could therefore explain this increased stiffness. Moreover, it has been demonstrated that an increase in mechanical load significantly reduced the collagen fiber crimp angle in the distal region of the Achilles tendon in rats undergoing moderate training.[64] Second, as PG content strongly increased at the enthesis after the reloading period, it is possible that these macromolecules play a role in the recovery of the elastic properties of the enthesis. Very recently, Abraham et al (2022)[18] reported increased stiffness of the mouse supraspinatus tendon enthesis as well as increased PG content after downhill treadmill training. In addition, in a rabbit model of rotator cuff anchor repair, PG content was positively correlated with tendon supraspinatus stiffness, 4 weeks of post-repair.[65] Further support is provided by the reported reduction in transverse compressive and axial tensile strains during ankle dorsiflexion, indicating a more rigid Achilles tendon enthesis, in patients with insertional Achilles tendinopathy[66] with, at the histological level, an increase in PG content.[67] The impact of PG on Achilles tendon stiffness is probably mediated by interactions of some of these macromolecules with collagens.[54,58] Finally, the greater CFc area observed in the HUR group than in the HU group could also contribute to the increase in enthesis stiffness. The studies of Schwartz et al. (2013)[34] and Schwartz et al. (2015)[68] strongly support this hypothesis. In a botulinum toxin unloading model[34] (Schwartz et al., 2013) and a model of cKO mice with a severe mineralization defect of the mineralized fibrocartilage,[68] the developing supraspinatus tendon enthesis showed both a significant decrease in enthesis stiffness and changes in the amount and/or quality of mineralized fibrocartilage.

Both in our biological and mechanical studies, there are some limitations. Except for the fibrocartilage surface area, biological parameters were qualitatively assessed. A semi-quantitative or quantitative approach would allow correlations between biological and mechanical parameters. Unfortunately, the mouse Achilles enthesis is very small in size which considerably limits the number of analyses on the same sample and consequently increases the number of animals needed. As a consequence, we chose to have multiple approaches, even if it was qualitative, to have a global overview of the adaptations. With regard to our mechanical analysis, we performed a video-based point tracking in order to obtain local stiffness values of the enthesis. Since the sample was very small, we chose to track only one point to characterize the enthesis displacements. For further investigation, a camera with better resolution could be used to study the enthesis strain pattern by digital image correlation. In addition, we were only able to compare the strength and stiffness parameters because we did not explore the geometry of the enthesis. For future work, non-destructive imaging techniques such as X-ray microtomography could be used prior to testing, in addition to video tracking, to analyze stress–strain curves and characterize the material properties of the enthesis.

5 | CONCLUSION

With increasing space exploration and the prospect of missions to Mars, it is more important than ever to know how microgravity can affect the musculoskeletal system, so as to prevent deleterious effects and to prepare astronauts for their return to Earth. While effects on muscle, bone, and tendon are well documented, few studies have examined the effects on the tendon-bone interface. Yet the enthesis deserves attention since enthesopathy-type pain has been reported by astronauts.[69] Our study showed that, despite structural remodeling affecting mainly the UFc of the enthesis, short exposure to simulated microgravity conditions coupled with a short period of free remobilization does not affect the tensile strength of the Achilles tendon enthesis. However, by reducing the stiffness of the tendon-bone interface, simulated microgravity conditions may impair force transmission between the Achilles tendon and the calcaneus. In addition, as compressive stress seems to be associated with the development of enthesopathies,[70] in-spaceflight, exercise countermeasures involving ankle dorsiflexion could lead to Achilles insertional tendinopathies by applying compressive stress to an enthesis that has lost

its protective fibrocartilaginous characteristics. To test these hypotheses, future work should address enthesis resistance to compressive stress under unloading. It will be instructive to determine whether the prophylactic measures usually prescribed to compensate for the deleterious effects of the microgravity environment on the musculoskeletal system are successful or not in maintaining the structural and functional integrity of the Achilles tendon enthesis.

AUTHOR CONTRIBUTIONS

Sandrine Roffino, Martine Pithioux, and Angèle Chopard conceived and designed the research. Théo Fovet and Thomas Brioche performed the animal procedure and the muscle atrophy assessment. Claire Camy, Sandrine Roffino, Alexandrine Bertaud, Edouard Lamy, Karim Senni, and Cécile Genovesio performed the biological experiments and interpreted the data. Claire Camy performed the biomechanical experiment and interpreted the data. Sandrine Roffino and Claire Camy wrote the manuscript. *All authors were involved in revising the manuscript*.

ACKNOWLEDGMENTS

We thank the animal facilities staff from the METAMUS platform, part of the "Montpellier animal facilities network" (RAM, BIOCAMPUS). We also thank Marylène LALLEMAND from the Mecabio Platform for her mechanical technical assistance and Marjorie SWEETKO for revising the English of the manuscript.

FUNDING INFORMATION

This study was funded by The French Centre National d'Etudes Spatiales (CNES), 4800000797.

DISCLOSURES

The authors declare no conflicts of interest.

DATA AVAILABILITY STATEMENT

The authors confirm that the data supporting the finding of this study are available within the article.

REFERENCES

1. Bloomfield SA, Martinez DA, Boudreaux RD, Mantri AV. Microgravity stress: bone and connective tissue. *Compr Physiol*. 2016;6(2):645-686.
2. Gao Y, Arfat Y, Wang H, Goswami N. Muscle atrophy induced by mechanical unloading: mechanisms and potential countermeasures. *Front Physiol*. 2018;9:235.
3. Lang T, Van Loon JJWA, Bloomfield S, et al. Towards human exploration of space: the THESEUS review series on muscle and bone research priorities. *NPJ Microgravity*. 2017;3:8.
4. Vico L, Hargens A. Skeletal changes during and after spaceflight. *Nat Rev Rheumatol*. 2018;14(4):229-245.
5. Almeida-Silveira MI, Lambertz D, Pérot C, Goubel F. Changes in stiffness induced by hindlimb suspension in rat Achilles tendon. *Eur J Appl Physiol*. 2000;81(3):252-257.
6. Deymier AC, Schwartz AG, Lim C, et al. Multiscale effects of spaceflight on murine tendon and bone. *Bone*. 2020;131:115152.
7. Kubo K, Akima H, Kouzaki M, et al. Changes in the elastic properties of tendon structures following 20 days bed-rest in humans. *Eur J Appl Physiol*. 2000;83(6):463-468.
8. Nakagawa Y, Totsuka M, Sato T, Fukuda Y, Hirota K. Effect of disuse on the ultrastructure of the achilles tendon in rats. *Eur J Appl Physiol Occup Physiol*. 1989;59(3):239-242.
9. Reeves ND, Maganaris CN, Ferretti G, Narici MV. Influence of 90-day simulated microgravity on human tendon mechanical properties and the effect of resistive countermeasures. *J Appl Physiol*. 2005;98(6):2278-2286.
10. Vailas AC, Deluna DM, Lewis LL, Curwin SL, Roy RR, Alford EK. Adaptation of bone and tendon to prolonged hindlimb suspension in rats. *J Appl Physiol*. 1988;65(1):373-376.
11. Friese N, Gierschner MB, Schadzek P, Roger Y, Hoffmann A. Regeneration of damaged tendon-bone junctions (entheses)—TAK1 as a potential node factor. *Int J Mol Sci*. 2020;21(15):5177.
12. Roffino S, Camy C, Foucault-Bertaud A, Lamy E, Pithioux M, Chopard A. Negative impact of disuse and unloading on tendon enthesis structure and function. *Life Sci Space Res*. 2021;29:46-52.
13. Rufai A, Ralphs JR, Benjamin M. Structure and histopathology of the insertional region of the human Achilles tendon. *J Orthop Res*. 1995;13(4):585-593.
14. Benjamin M, Evans EJ. Fibrocartilage. *J Anat*. 1990;171:1-15.
15. Cury DP, Dias FJ, Miglino MA, Watanabe I. Structural and ultrastructural characteristics of bone-tendon junction of the calcaneal tendon of adult and elderly Wistar rats. *PLoS One*. 2016;11(4):e0153568.
16. Genin GM, Kent A, Birman V, et al. Functional grading of mineral and collagen in the attachment of tendon to bone. *Biophys J*. 2009;97(4):976-985.
17. Shaw HM, Benjamin M. Structure-function relationships of entheses in relation to mechanical load and exercise. *Scand J Med Sci Sports*. 2007;17(4):303-315.
18. Abraham AC, Fang F, Golman M, Oikonomou P, Thomopoulos S. The role of loading in murine models of rotator cuff disease. *J Orthop Res*. 2022;40(4):977-986.
19. Kannus P, Jozsa L, Kvist M, et al. Expression of osteocalcin in the patella of experimentally immobilized and remobilized rats. *J Bone Miner Res*. 1996;11(1):79-87.
20. Deymier AC, Schwartz AG, Cai Z, et al. The multiscale structural and mechanical effects of mouse supraspinatus muscle unloading on the mature enthesis. *Acta Biomater*. 2019;83:302-313.
21. Frizziero A, Fini M, Salamanna F, Veicsteinas A, Maffulli N, Marini M. Effect of training and sudden detraining on the patellar tendon and its enthesis in rats. *BMC Musculoskelet Disord*. 2011;12:20.
22. Jarvinen TA, Jozsa L, Kannus P, et al. Mechanical loading regulates tenascin-C expression in the osteotendinous junction. *J Cell Sci*. 1999;112(18):3157-3166.
23. Mutsuzaki H, Nakajima H, Wadano Y, Takahashi H, Sakane M. Influence of mechanical unloading on histological

changes of the patellar tendon insertion in rabbits. *Knee*. 2015;22(6):469-474.
24. Shen H, Lim C, Schwartz AG, Andreev-Andrievskiy A, Deymier AC, Thomopoulos S. Effects of spaceflight on the muscles of the murine shoulder. *FASEB J*. 2017;31(12):5466-5477.
25. Morey-Holton ER, Globus RK. Hindlimb unloading rodent model: technical aspects. *J Appl Physiol*. 2002;92(4):1367-1377.
26. Amblard D, Lafage-Proust M-H, Laib A, et al. Tail suspension induces bone loss in skeletally mature mice in the C57BL/6J strain but not in the C3H/HeJ strain. *J Bone Miner Res*. 2003;18(3):561-569.
27. Koike Y, Trudel G, Uhthoff HK. Formation of a new enthesis after attachment of the supraspinatus tendon: a quantitative histologic study in rabbits. *J Orthop Res*. 2005;23(6):1433-1440.
28. Junqueira LCU, Bignolas G, Brentani RR. Picrosirius staining plus polarization microscopy, a specific method for collagen detection in tissue sections. *Histochem J*. 1979;11(4):447-455.
29. Kirstein B, Chambers TJ, Fuller K. Secretion of tartrate-resistant acid phosphatase by osteoclasts correlates with resorptive behavior. *J Cell Biochem*. 2006;98(5):1085-1094.
30. Knowles HJ, Moskovsky L, Thompson MS, et al. Chondroclasts are mature osteoclasts which are capable of cartilage matrix resorption. *Virchows Arch*. 2012;461(2):205-210.
31. Best TM, Collins A, Lilly EG, Seaber AV, Goldner R, Murrell GAC. Achilles tendon healing: a correlation between functional and mechanical performance in the rat. *J Orthop Res*. 1993;11(6):897-906.
32. Hanson AM, Harrison BC, Young MH, Stodieck LS, Ferguson VL. Longitudinal characterization of functional, morphologic, and biochemical adaptations in mouse skeletal muscle with hindlimb suspension. *Muscle Nerve*. 2013;48(3):393-402.
33. Chimenti RL, Flemister AS, Ketz J, Bucklin M, Buckley MR, Richards MS. Ultrasound strain mapping of Achilles tendon compressive strain patterns during dorsiflexion. *J Biomech*. 2016;49(1):39-44.
34. Schwartz AG, Lipner JH, Pasteris JD, Genin GM, Thomopoulos S. Muscle loading is necessary for the formation of a functional tendon enthesis. *Bone*. 2013;55(1):44-51.
35. Benjamin M, Newell RL, Evans EJ, Ralphs JR, Pemberton DJ. The structure of the insertions of the tendons of biceps brachii, triceps and brachialis in elderly dissecting room cadavers. *J Anat*. 1992;180(Pt 2):327-332.
36. Frowen P, Benjamin M. Variations in the quality of uncalcified fibrocartilage at the insertions of the extrinsic calf muscles in the foot. *J Anat*. 1995;186(Pt 2):417-421.
37. Jensen PT, Lambertsen KL, Frich LH. Assembly, maturation, and degradation of the supraspinatus enthesis. *J Shoulder Elbow Surg*. 2018;27(4):739-750.
38. Waggett AD, Ralphs JR, Kwan APL, Woodnutt D, Benjamin M. Characterization of collagens and proteoglycans at the insertion of the human achilles tendon. *Matrix Biol*. 1998;16(8):457-470.
39. Juneja SC, Veillette C. Defects in tendon, ligament, and enthesis in response to genetic alterations in key proteoglycans and glycoproteins: a review. *Art Ther*. 2013;2013:154812.
40. Leyden J, Kaizawa Y, Chang J. Principles of tendon regeneration. In: Duscher D, Shiffman MA, eds. *Regenerative Medicine and Plastic Surgery: Skin and Soft Tissue, Bone, Cartilage, Muscle, Tendon and Nerves [Internet]*. Springer International Publishing; 2019:355-367.
41. Chen S, Fu P, Wu H, Pei M. Meniscus, articular cartilage and nucleus pulposus: a comparative review of cartilage-like tissues in anatomy, development and function. *Cell Tissue Res*. 2017;370(1):53-70.
42. Hutton WC, Yoon ST, Elmer WA, et al. Effect of tail suspension (or simulated weightlessness) on the lumbar intervertebral disc: study of proteoglycans and collagen. *Spine*. 2002;27(12):1286-1290.
43. Kwok AT, Mohamed NS, Plate JF, et al. Spaceflight and hind limb unloading induces an arthritic phenotype in knee articular cartilage and menisci of rodents. *Sci Rep*. 2021;11(1):10469.
44. Yasuoka H, Asazuma T, Nakanishi K, et al. Effects of reloading after simulated microgravity on proteoglycan metabolism in the nucleus pulposus and anulus fibrosus of the lumbar intervertebral disc: an experimental study using a rat tail suspension model. *Spine*. 2007;32(25):E734-E740.
45. Potter R, Havlioglu N, Thomopoulos S. The developing shoulder has a limited capacity to recover after a short duration of neonatal paralysis. *J Biomech*. 2014;47(10):2314-2320.
46. Iandolo D, Strigini M, Guignandon A, Vico L. Osteocytes and weightlessness. *Curr Osteoporos Rep*. 2021;19(6):626-636.
47. Sone T, Imai Y, Tomomitsu T, Fukunaga M. Calcaneus as a site for the assessment of bone mass. *Bone*. 1998;22(5 Suppl):155S-157S.
48. Gerbaix M, White H, Courbon G, Shenkman B, Gauquelin-Koch G, Vico L. Eight days of earth Reambulation worsen bone loss induced by 1-month spaceflight in the major weight-bearing ankle bones of mature mice. *Front Physiol*. 2018;9:746.
49. Zheng P, Chen R, Liu H, et al. On the standards and practices for miniaturized tensile test—a review. *Fusion Eng Des*. 2020;161:112006.
50. Perrier A, Touchard F, Chocinski-Arnault L, Mellier D. Quantitative analysis by micro-CT of damage during tensile test in a woven hemp/epoxy composite after water ageing. *Compos A Appl Sci Manuf*. 2017;102:18-27.
51. Golman M, Abraham AC, Kurtaliaj I, et al. Toughening mechanisms for the attachment of architectured materials: the mechanics of the tendon enthesis. *Sci Adv*. 2021;7(48):eabi5584.
52. Gerbaix M, Gnyubkin V, Farlay D, et al. One-month spaceflight compromises the bone microstructure, tissue-level mechanical properties, osteocyte survival and lacunae volume in mature mice skeletons. *Sci Rep*. 2017;7(1):2659.
53. Matsumoto F, Trudel G, Uhthoff HK, Backman DS. Mechanical effects of immobilization on the Achilles' tendon. *Arch Phys Med Rehabil*. 2003;84(5):662-667.
54. Eisner LE, Rosario R, Andarawis-Puri N, Arruda EM. The role of the non-collagenous extracellular matrix in tendon and ligament mechanical behavior: a review. *J Biomech Eng*. 2022;144(5):050801.
55. Minns RJ, Soden PD, Jackson DS. The role of the fibrous components and ground substance in the mechanical properties of biological tissues: a preliminary investigation. *J Biomech*. 1973;6(2):153-165.
56. Eleswarapu SV, Responte DJ, Athanasiou KA. Tensile properties, collagen content, and crosslinks in connective tissues of the immature knee joint. *PLoS One*. 2011;6(10):e26178.
57. Rigozzi S, Müller R, Snedeker JG. Local strain measurement reveals a varied regional dependence of tensile tendon mechanics on glycosaminoglycan content. *J Biomech*. 2009;42(10):1547-1552.

58. Thorpe CT, Birch HL, Clegg PD, Screen HRC. The role of the non-collagenous matrix in tendon function. *Int J Exp Path*. 2013;94(4):248-259.
59. Lyman J, Weinhold PS, Almekinders LC. Strain behavior of the distal Achilles tendon: implications for insertional Achilles tendinopathy. *Am J Sports Med*. 2004;32(2):457-461.
60. Krause AR, Speacht TA, Steiner JL, Lang CH, Donahue HJ. Mechanical loading recovers bone but not muscle lost during unloading. *NPJ Microgravity*. 2020;6(1):1-8.
61. Basso N, Jia Y, Bellows CG, Heersche JNM. The effect of reloading on bone volume, osteoblast number, and osteoprogenitor characteristics: studies in hind limb unloaded rats. *Bone*. 2005;37(3):370-378.
62. Thomopoulos S, Kim H-M, Rothermich SY, Biederstadt C, Das R, Galatz LM. Decreased muscle loading delays maturation of the tendon enthesis during postnatal development. *J Orthop Res*. 2007;25(9):1154-1163.
63. Spiesz EM, Thorpe CT, Thurner PJ, Screen HRC. Structure and collagen crimp patterns of functionally distinct equine tendons, revealed by quantitative polarised light microscopy (qPLM). *Acta Biomater*. 2018;70:281-292.
64. Franchi M, Torricelli P, Giavaresi G, Fini M. Role of moderate exercising on Achilles tendon collagen crimping patterns and proteoglycans. *Connect Tissue Res*. 2013;54(4–5):267-274.
65. Campbell TM, Gao L, Laneuville O, Louati H, Uhthoff HK, Trudel G. Rotator cuff anchor repair: histological changes associated with the recovering mechanical properties in a rabbit model. *J Tissue Eng Regen Med*. 2021;15(6):567-576.
66. Chimenti RL, Bucklin M, Kelly M, et al. Insertional achilles tendinopathy associated with altered transverse compressive and axial tensile strain during ankle dorsiflexion. *J Orthop Res*. 2017;35(4):910-915.
67. Maffulli N, Reaper J, Ewen SWB, Waterston SW, Barrass V. Chondral metaplasia in calcific insertional tendinopathy of the Achilles tendon. *Clin J Sport Med*. 2006;16(4):329-334.
68. Schwartz AG, Long F, Thomopoulos S. Enthesis fibrocartilage cells originate from a population of hedgehog-responsive cells modulated by the loading environment. *Development*. 2015;142(1):196-206.
69. Shackelford LC, LeBlanc AD, Driscoll TB, et al. Resistance exercise as a countermeasure to disuse-induced bone loss. *J Appl Physiol*. 2004;97(1):119-129.
70. Maganaris CN, Narici MV, Almekinders LC, Maffulli N. Biomechanics and pathophysiology of overuse tendon injuries. *Sports Med*. 2004;34(14):1005-1017.

How to cite this article: Camy C, Brioche T, Senni K, et al. Effects of hindlimb unloading and subsequent reloading on the structure and mechanical properties of Achilles tendon-to-bone attachment. *The FASEB Journal*. 2022;00:e22548. doi: 10.1096/fj.202200713R